SEMARAK ILMU PUBLISHING

Journal of Advanced Research in Fluid Mechanics and Thermal Sciences

Journal homepage:
https://semarakilmu.com.my/journals/index.php/fluid_mechanics_thermal_sciences/index
ISSN: 2289-7879

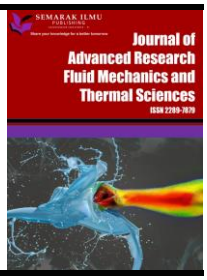

Influence of Cavity on Base Pressure Manipulation in Suddenly Expanded Flow from Converging Diverging Nozzle for Area Ratio 5.29

Ridwan[1], Sher Afghan Khan[1,*], Jaffar Syed Mohamed Ali[1], Mohd. Azan Mohammed Sapardi[1]

[1] Mechanical and Aerospace Engineering Department, Faculty of Engineering, International Islamic University, Kuala Lumpur, 53100, Malaysia

ARTICLE INFO

Article history:
Received 15 October 2023
Received in revised form 16 January 2024
Accepted 29 January 2024
Available online 29 February 2024

Keywords:
Base pressure; cavity; Mach number; nozzle pressure ratio

ABSTRACT

This study delves into the intricate interplay of cavity placement, Nozzle Pressure Ratio (NPR), and Mach numbers, examining their collective influence on manipulating base pressure within a duct. Employing numerical simulations, the research explores the cavity's effectiveness in altering base pressure dynamics in the duct's base area. The investigation comprehensively studies various factors, including length-to-diameter ratio, nozzle pressure ratio, Mach number, and cavity location. The simulations are conducted for a singular cavity at multiple positions concerning the duct's diameter, maintaining a fixed cavity width-to-height ratio of 1. The NPR ranges from 2 to 8, and the Mach numbers under scrutiny span from 1.2 to 1.8. The study meticulously analyses variations in base pressure and alterations in the pressure field resulting from these variables. Notably, the findings demonstrate the cavity's adeptness in controlling base pressure, particularly at NPR values of 4 and 6 for Mach numbers 1.2 and 1.4. In contrast, ineffectiveness is observed at NPR 2 and 8 due to specific flow reattachment points. However, the cavity effectively influences base pressure at NPR values of 4, 6, and 8 for Mach numbers 1.6 and 1.8. These discernments offer invaluable insights for the optimization of duct designs in diverse engineering applications.

1. Introduction

Nozzles serve a pivotal role in a myriad of industrial applications by accelerating fluids into high-speed jets, essential for fuel injectors, water jet cutting machines, and sprays. The versatile utility of these nozzles in both industrial and consumer goods sectors underscores their significance. Particularly, converging-diverging (CD) nozzles are crucial, capable of accelerating fluids to speeds surpassing the sound barrier, and generating maximal thrust. In aerospace industries, CD nozzles power supersonic jets, vital for satellite launches and space vehicle propulsion.

The endeavor to control base pressure has been a driving force behind extensive research in the realm of suddenly extended flows [1]. Researchers have predominantly favored passive control methods due to their autonomy from specific external systems, unlike their active control counterparts. These methods encompass analytical examinations of both internal and external flows

* *Corresponding author.*
E-mail address: sakhan@iium.edu.my

https://doi.org/10.37934/arfmts.114.2.3249

[2]. The shape of the object should be streamlined to minimize the drag [3,4]. The various parameters affecting suddenly expanded flows have been studied by Pathan *et al.,* [5,6]. The length of the enlarged duct is optimized by Pathan *et al.,* [7]. The area ratio should be optimum to generate more thrust by the convergent divergent nozzle [8]. The effect on parameters Mach number, area ratio, and NPR are studied and found that these parameters are influencing parameters to change base pressure and the thrust [9-11]. The literature extensively documents studies related to suddenly expanded flow problems, further enriching our understanding [12]. Passive techniques predominantly involve geometric modifications, such as integrating cavities and ribs within extended ducts. Notably, these methods are easier to fabricate and thus more cost-effective. Among the widely employed passive control strategies, cavities and ribs stand out prominently [13,14].

Simultaneously, active control techniques have been explored, involving methods like control jets to augment base pressure [15,16]. Analytical studies utilizing Computational Fluid Dynamics (CFD) analysis have meticulously examined external flows over 2D wedges, 3D cones, and catalytic converters, yielding promising results [17-19]. CFD analysis is widely used in various applications and similar studies have been found in the literature using CFD analysis [20-28].

While existing literature presents an array of studies on high-velocity flows incorporating both active and passive control methods, there exists a specific research gap. While active and passive control methods have been thoroughly investigated and utilized in various applications, a comprehensive exploration focusing specifically on cavities as a passive control approach is relatively scarce. This research paper aims to address this gap by delving into the intricacies of employing cavities as a method of passive flow control at various locations concerning the duct diameter, offering a unique perspective and expanding the existing knowledge base in this domain.

2. CFD Analysis

In the context of boundary conditions, the inlet is defined as a velocity inlet, while the outlet is specified as a pressure outlet. Figure 1 shows the geometry and boundary conditions. The determination of inlet velocities is contingent upon varying Mach numbers, meticulously calculated and assigned at the inlet boundary. Notably, the outlet pressure is precisely set to zero-gauge pressure. For the computational solver utilized in this study, a density-based approach was adopted, as opposed to a pressure-based one. This choice was made to comprehensively account for compressibility effects and the diverse inertia levels inherent in the analysis, as emphasized in prior research [29,30].

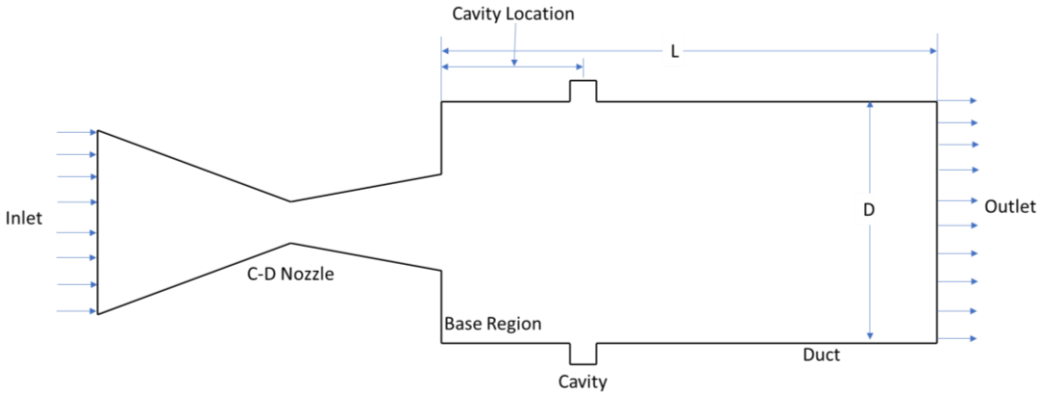

Fig. 1. Nozzle and an enlarged duct

The selection of an appropriate turbulence model is of paramount importance in Computational Fluid Dynamics (CFD) analyses. In this study, the k-ε turbulence model was consistently applied for the entirety of the analysis. To ensure the highest level of precision in the results, a stringent error tolerance of 10^{-6} was set, and iterations were meticulously continued until solution convergence was achieved. This rigorous approach to convergence was undertaken, following established guidelines and corroborated by previous studies [2-5,8-12].

In this research, specific parameters have been carefully determined to maintain consistency and accuracy throughout the simulations. The area ratio, a crucial factor, is kept constant at 5.29, forming a foundational element of the study. Additionally, the width-to-height ratio of the cavity under investigation is set at 1 (3:3), a dimension meticulously chosen for detailed Computational Fluid Dynamics (CFD) analysis. Table 1 presents a comprehensive overview of the factors and their corresponding levels, outlining the variables under consideration.

For this study, the CFD analysis is conducted for multiple cases, both with the inclusion of the cavity and without it. This comparative analysis is instrumental in elucidating the impact of the cavity on the flow dynamics within the given system. By systematically considering these variations, the research aims to draw significant conclusions about the efficacy of the cavity as a passive flow control mechanism.

Table 1
Factors and levels

Parameters	Level 1	Level 2	Level 3	Level 4
Nozzle pressure ratio (NPR)	2	4	6	8
Length to diameter ratio (L/D)	3	4	5	6
Mach No. (M)	1.2	1.4	1.6	1.8
Location of Cavity (C)	0.5D	1D	1.5D	2D
	11.5 mm	23 mm	34.5 mm	46 mm

The variables under scrutiny in this investigation encompass Nozzle Pressure Ratio (N), Mach Number (M), Cavity Location (C), and Length-to-Diameter Ratio (L). Within this framework, the enlarged duct diameter (D) remains constant at 20 mm, while the diameter at the nozzle outlet is consistently set at 10 mm. The dimensions of the nozzle are meticulously calculated for diverse Mach numbers and are comprehensively outlined in Table 2. To facilitate the analysis, these geometries are meticulously modeled using ANSYS Workbench and rigorously examined within the Fluent software environment.

Table 2
Dimensions of the nozzle (in mm)

Parameters	Mach No.			
	1.2	1.4	1.6	1.8
Inlet Diameter (Di)	20.57	20.19	22.34	21.73
Exit Diameter (De)	10.00	10.00	10.00	10.00
Throat Diameter (Dt)	9.85	9.47	8.94	8.34
Diverging Length (Ld)	8.53	10.11	10.08	9.51
Converging Length (Lc)	20.00	20.00	25.00	25.00

The three-dimensional model is meticulously meshed using the ANSYS Workbench, employing a hexahedral meshing scheme. The dimensions of the grid segments play a pivotal role in this Computational Fluid Dynamics (CFD) investigation, significantly influencing its accuracy and computational efficiency. Achieving precise results within the shortest computation period hinges on

optimizing the element size. To achieve this, a grid independence test is rigorously conducted, spanning grid element dimensions from 0.1 mm to 5 mm. The objective is to identify the optimal element size that ensures accuracy without compromising computational efficiency.

The outcomes of the grid independence test, as detailed in Table 3, reveal the stability of results when utilizing a grid element size of 1 mm. Consequently, for further CFD analysis, a grid element size of 0.5 mm is judiciously selected, ensuring a balance between accuracy and computational expediency.

Table 3
Grid independence test

Mesh Element Size in mm	Mesh Nodes	Mesh Elements	Base Pressure
5	2796	652	0.584236
4	2807	720	0.659293
3	3087	1398	0.747249
2	6520	7884	0.623724
1	36110	55650	0.330512
0.5	243697	442519	0.331631
0.25	1955690	6587205	0.332747
0.1	25582028	12731891	0.333865

3. Results and Discussion

The base pressure values obtained from Fluent simulations are presented as gauge pressure. To enhance visualization and comprehension, these values are transformed into dimensionless pressure units. Converting the base pressure to a dimensionless form facilitates a clearer understanding of the results. Additionally, pressure contours are extracted from Fluent software and visually represented in Figure 1 to Figure 20, providing a graphical representation of the pressure distribution for detailed analysis.

3.1 Results: Pressure Contours

The pressure contours are depicted for a length-to-diameter ratio of 6, encompassing nozzle pressure ratios ranging from 2 to 8, and Mach numbers spanning from 1.2 to 1.8. Figure 1 to Figure 20 visually represent total pressure contours for various scenarios.

3.1.1 Pressure contours: Mach no. = 1.4, L/D = 6 and NPR = 2

Figure 2 to Figure 6 present pressure contours for a length-to-diameter ratio of 6, a Mach number of 1.4, and a nozzle pressure ratio of 2. These figures showcase pressure contours for cases both without a cavity and with a cavity placed at different locations, namely 0.5D, 1D, 1.5D, and 2D from the nozzle exit.

Upon close examination of Figure 2 to Figure 6, it becomes apparent that the flow from the converging-diverging (CD) nozzle experiences over-expansion. To achieve proper nozzle expansion at Mach number 1.4, a nozzle pressure ratio of 3.18 is necessary. Additionally, the contour analysis reveals that the reattachment distance, indicating the distance from the nozzle exit to the point where the flow attaches back to the duct, is approximately twice the diameter of the duct.

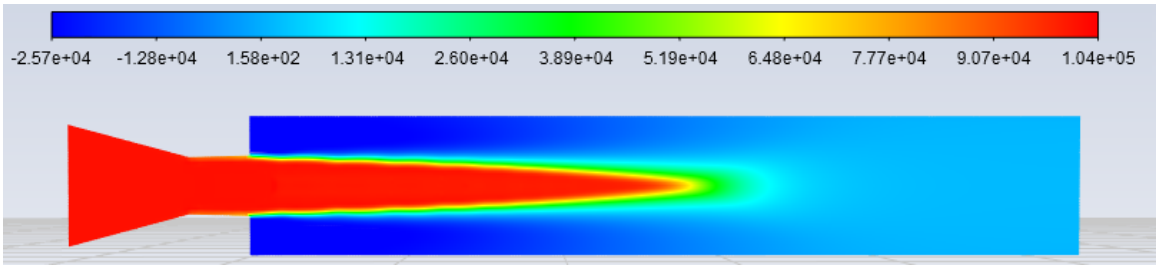

Fig. 2. Pressure contours: Mach No. = 1.4, L/D = 6, NPR = 2 and without cavity

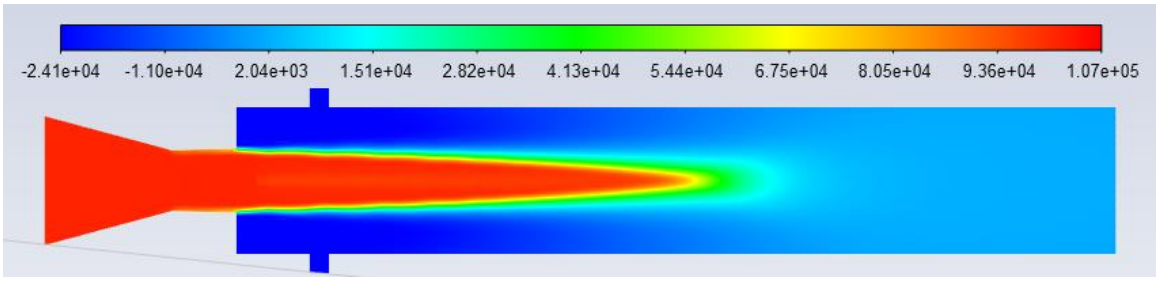

Fig. 3. Pressure contours: Mach No. = 1.4, L/D = 6, NPR = 2 and cavity at 0.5D

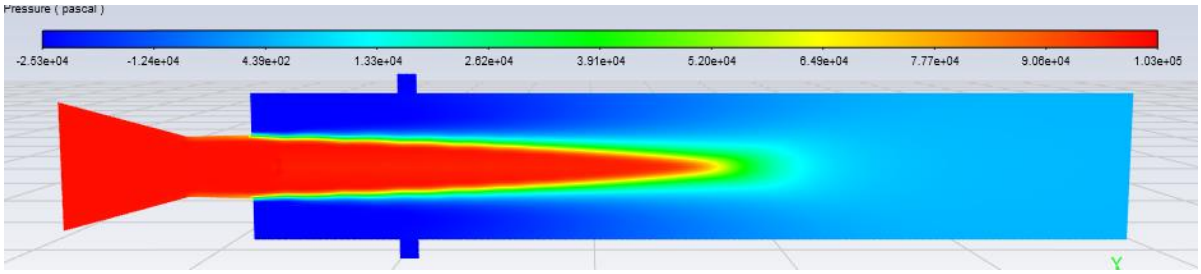

Fig. 4. Pressure contours: Mach No. = 1.4, L/D = 6, NPR = 2 and cavity at 1D

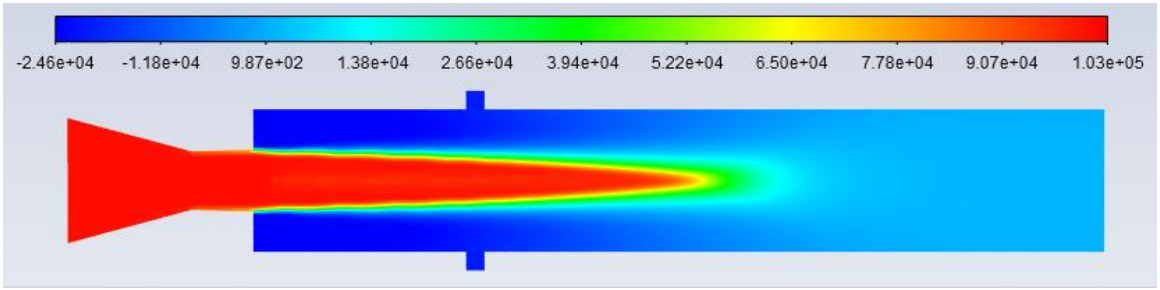

Fig. 5. Pressure contours: Mach No. = 1.4, L/D = 6, NPR = 2 and cavity at 1.5D

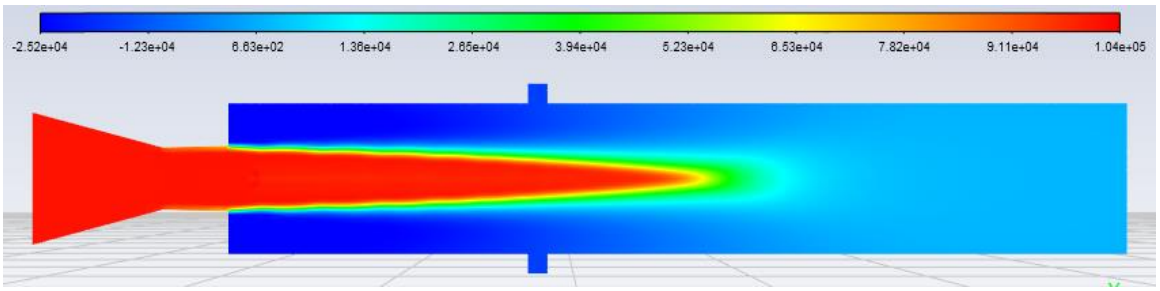

Fig. 6. Pressure contours: Mach No. = 1.4, L/D = 6, NPR = 2 and cavity at 2D

3.1.2 Pressure contours: Mach no. = 1.4, L/D = 6 and NPR = 4

Figure 7 to Figure 11 showcase the pressure contours corresponding to a length-to-diameter ratio of six, a Mach number of 1.4, and a nozzle pressure ratio of 4. These figures present pressure contours for scenarios without a cavity and with a cavity placed at different locations: 0.5D, 1D, 1.5D, and 2D from the nozzle exit.

Upon careful observation of Figure 7 to Figure 11, it becomes evident that the flow from the converging-diverging (CD) nozzle experiences under-expansion. To achieve proper nozzle expansion at Mach number 1.4, a nozzle pressure ratio of 3.18 is necessary, as indicated by the figures. Furthermore, the contour analysis reveals that the reattachment distance, denoting the distance from the nozzle exit to the point where the flow reattaches to the duct, is approximately half the diameter of the duct.

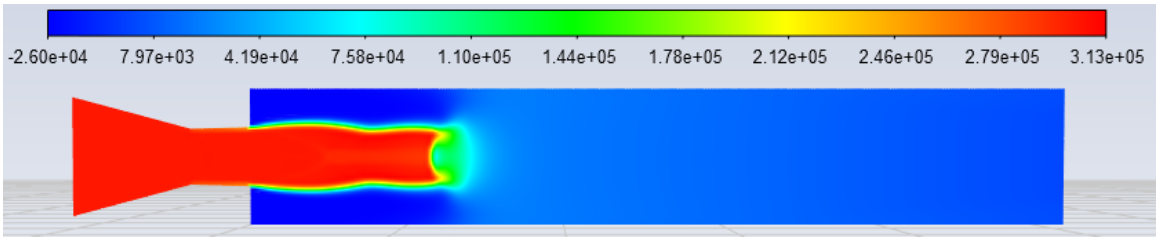

Fig. 7. Pressure contours: Mach No. = 1.4, L/D = 6, NPR = 4 and without cavity

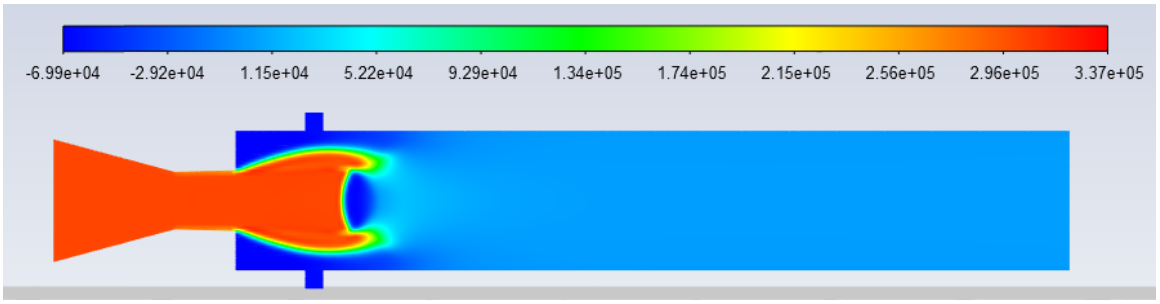

Fig. 8. Pressure contours: Mach No. = 1.4, L/D = 6, NPR = 4 and cavity at 0.5D

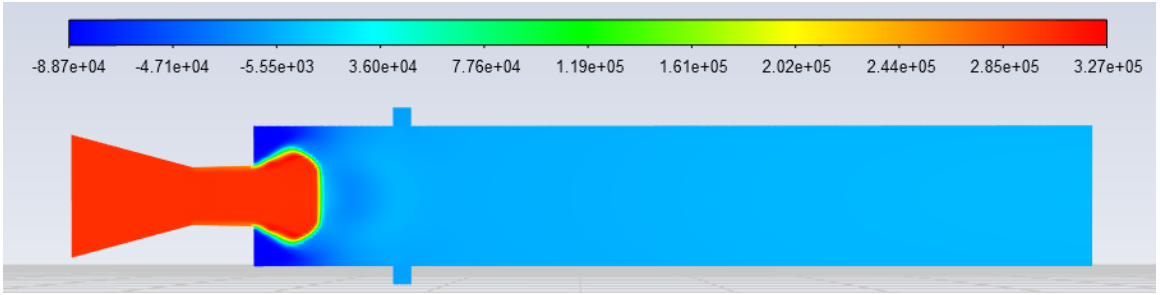

Fig. 9. Pressure contours: Mach No. = 1.4, L/D = 6, NPR = 4 and cavity at 1D

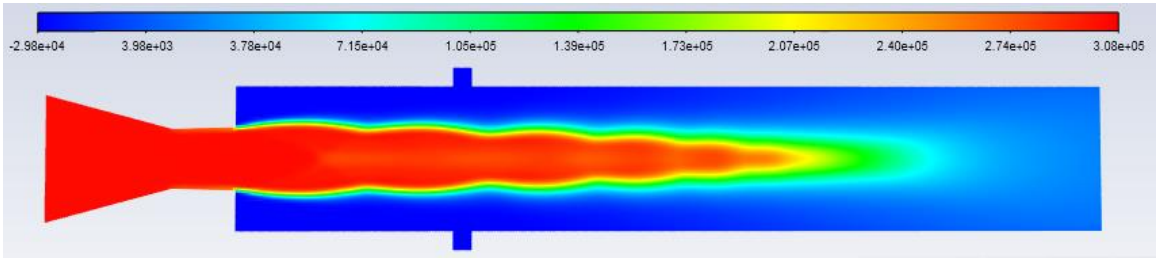

Fig. 10. Pressure contours: Mach No. = 1.4, L/D = 6, NPR = 4 and cavity at 1.5D

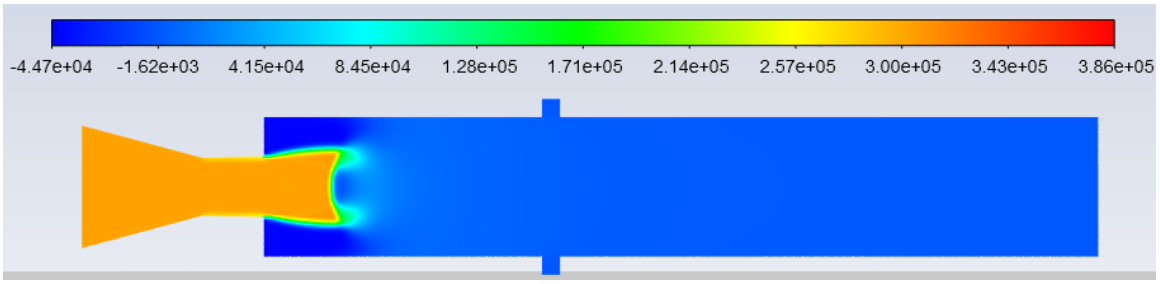

Fig. 11. Pressure contours: Mach No. = 1.4, L/D = 6, NPR = 4 and cavity at 2D

3.1.3 Pressure contours: Mach no. = 1.4, L/D = 6 and NPR = 6

Figure 12 to Figure 16 exhibit the pressure contours for a length-to-diameter ratio of six, a Mach number of 1.4, and a nozzle pressure ratio of 6. These figures illustrate pressure contours for cases without a cavity and with a cavity placed at various positions: 0.5D, 1D, 1.5D, and 2D from the nozzle exit.

Upon analysis of Figure 12 to Figure 16, it becomes evident that the flow from the converging-diverging (CD) nozzle experiences under-expansion. Achieving proper nozzle expansion at Mach number 1.4 necessitates a nozzle pressure ratio of 3.18, as indicated by the figures. Additionally, the contour analysis highlights that the reattachment distance, indicating the duct's distance from the nozzle exit to the point where the flow reattaches to the duct, is approximately half the diameter of the duct.

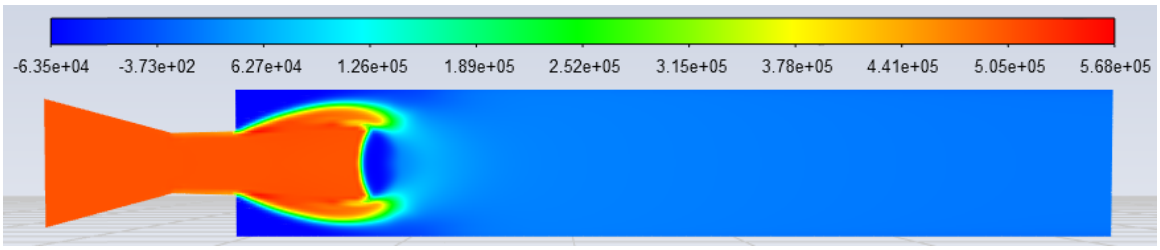

Fig. 12. Pressure contours: Mach No. = 1.4, L/D = 6, NPR = 6 and without cavity

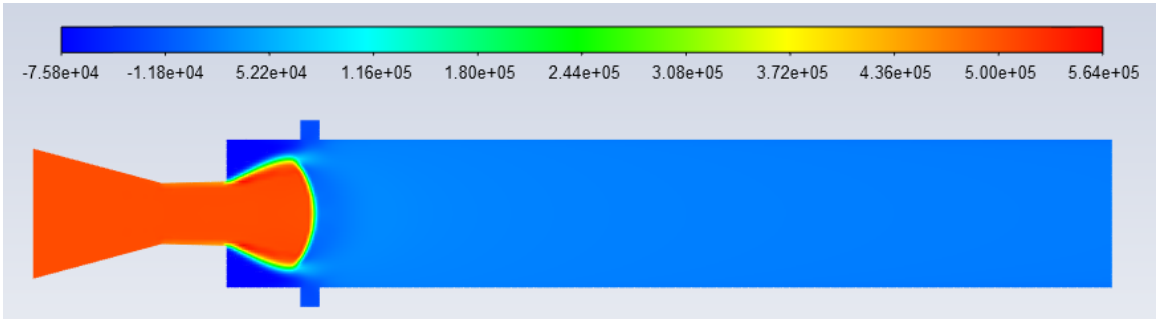

Fig. 13. Pressure contours: Mach No. = 1.4, L/D = 6, NPR = 6 and cavity at 0.5D

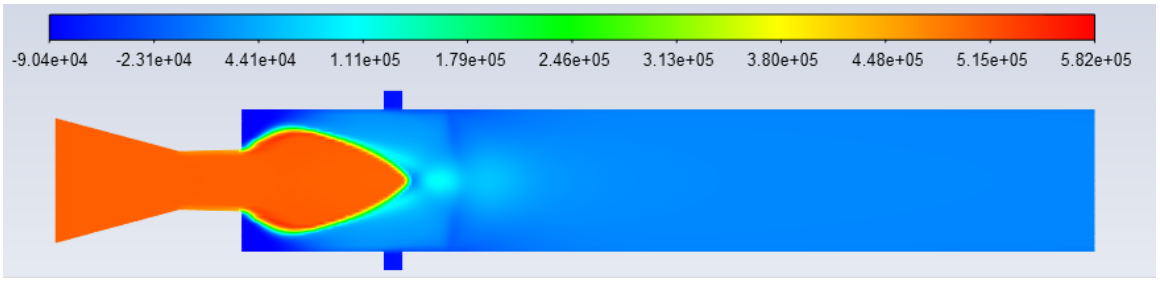

Fig. 14. Pressure contours: Mach No. = 1.4, L/D = 6, NPR = 6 and cavity at 1D

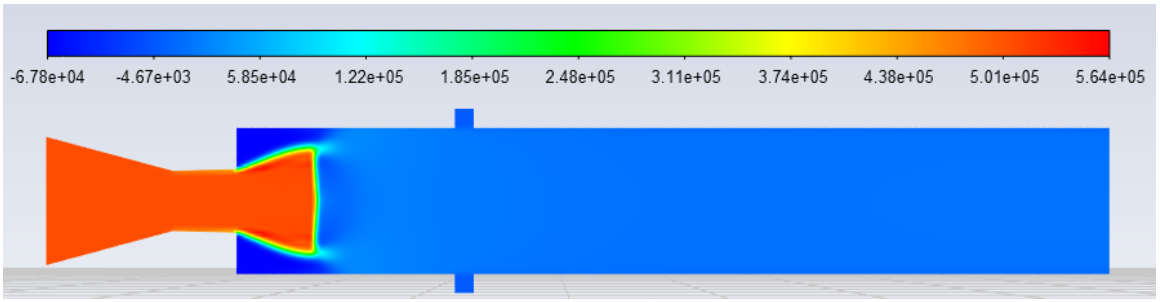

Fig. 15. Pressure contours: Mach No. = 1.4, L/D = 6, NPR = 6 and cavity at 1.5D

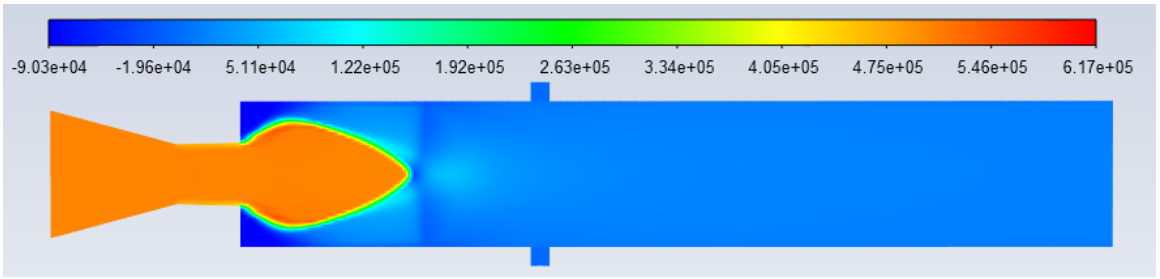

Fig. 16. Pressure contours: Mach No. = 1.4, L/D = 6, NPR = 6 and cavity at 2D

3.1.4 Pressure contours: Mach no. = 1.4, L/D = 6 and NPR = 8

Figure 17 to Figure 21 present pressure contours for a length-to-diameter ratio of six, a Mach number of 1.4, and a nozzle pressure ratio of 8. These figures illustrate pressure distributions for cases without a cavity and with a cavity placed at varying positions: 0.5D, 1D, 1.5D, and 2D from the nozzle exit.

Upon scrutiny of Figure 17 to Figure 21, it becomes evident that the flow from the converging-diverging (CD) nozzle experiences significant under-expansion. The contour analysis also reveals that the reattachment distance, indicating the duct's distance from the nozzle exit to the point where the flow reattaches to the duct, is roughly half the diameter of the duct.

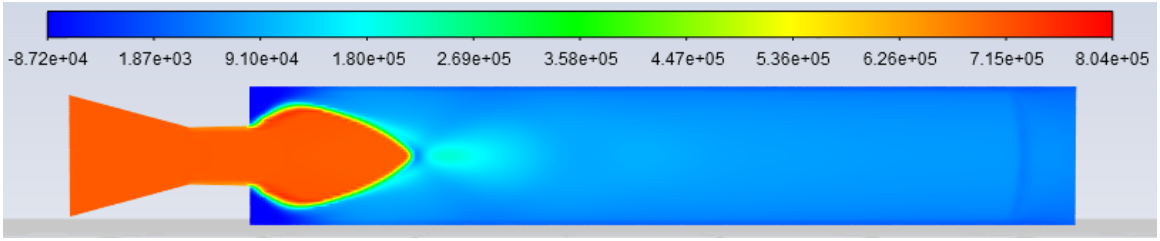

Fig. 17. Pressure contours: Mach No. = 1.4, L/D = 6, NPR = 8 and without cavity

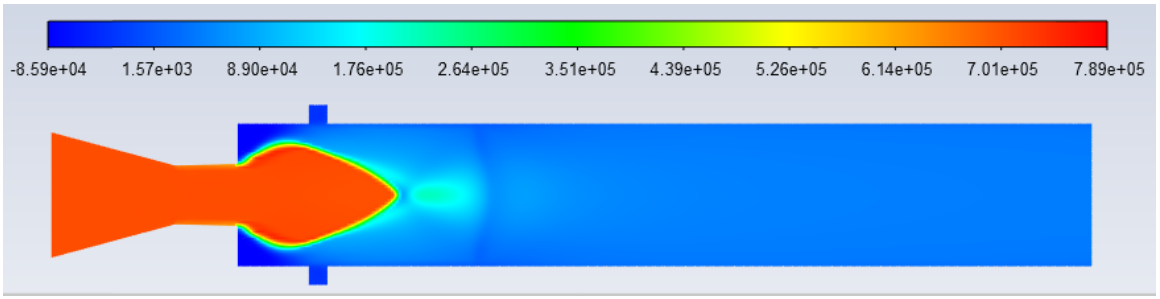

Fig. 18. Pressure contours: Mach No. = 1.4, L/D = 6, NPR = 8 and cavity at 0.5D

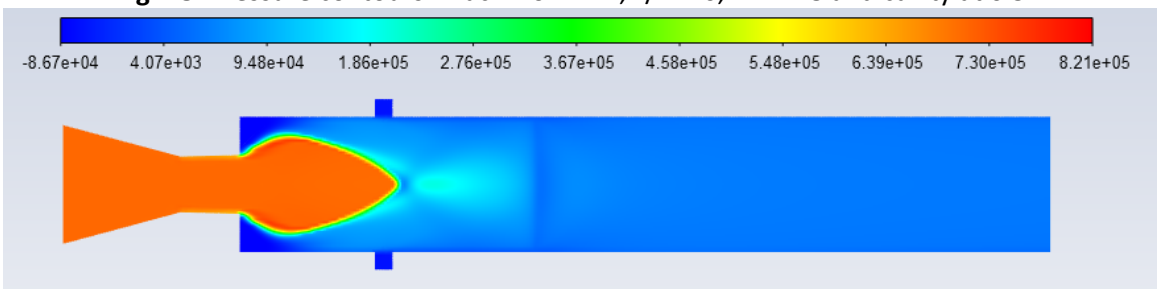

Fig. 19. Pressure contours: Mach No. = 1.4, L/D = 6, NPR = 8 and cavity at 1D

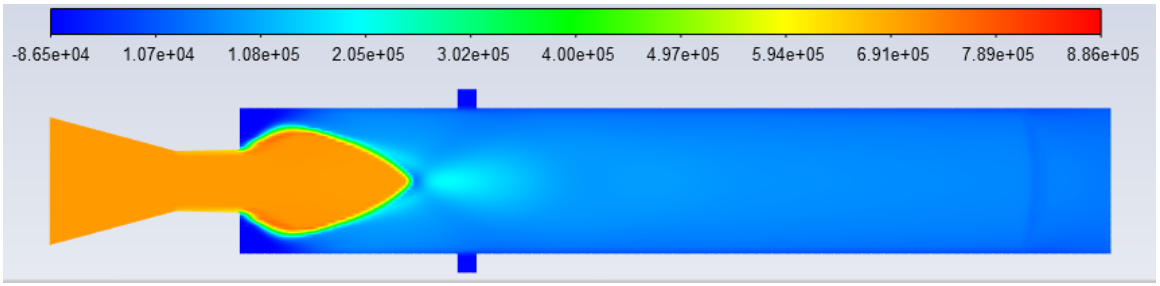

Fig. 20. Pressure contours: Mach No. = 1.4, L/D = 6, NPR = 8 and cavity at 1.5D

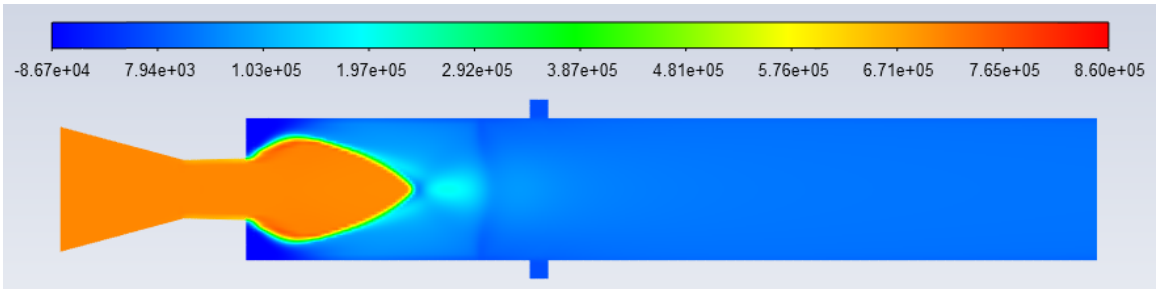

Fig. 21. Pressure contours: Mach No. = 1.4, L/D = 6, NPR = 8 and cavity at 2D

3.2 Results: Base Pressure for Mach No. 1.2

Figure 22 to Figure 25 present the analysis of base pressure variations considering different parameters, including nozzle pressure ratios, presence or absence of a cavity, and various cavity locations, all for a Mach number of 1.2.

The observations from Figure 22 to Figure 25 indicate the efficacy of the cavity in manipulating the base pressure. Specifically, at nozzle pressure ratios of four and six, the cavity proves beneficial in altering the base pressure. Notably, when the nozzle pressure ratio is set at six, the cavity demonstrates consistent effectiveness in augmenting the base pressure across all locations, including 0.5D, 1D, 1.5D, and 2D. Particularly at the 0.5D location, the cavity exhibits a significant impact on

base pressure enhancement. However, for nozzle pressure ratios of two and eight, the influence of the cavity on base pressure remains negligible, with minimal differences observed in the outcomes.

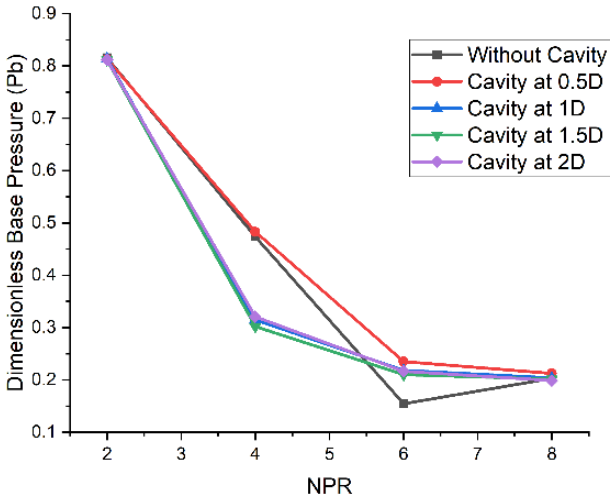

Fig. 22. Base pressure Vs NPR for Mach number 1.2 and L/D 3

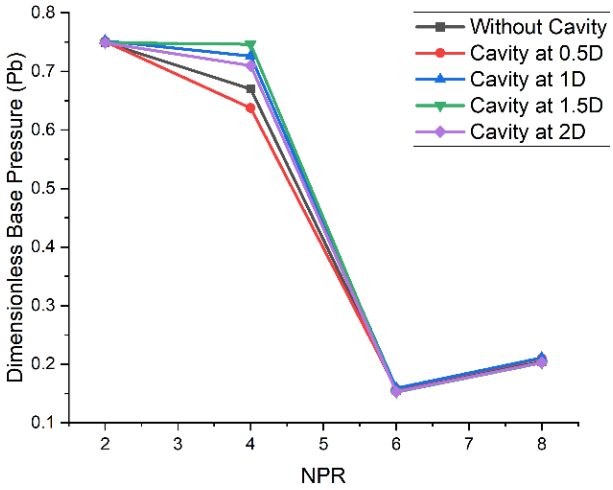

Fig. 23. Base pressure Vs NPR for Mach number 1.2 and L/D 4

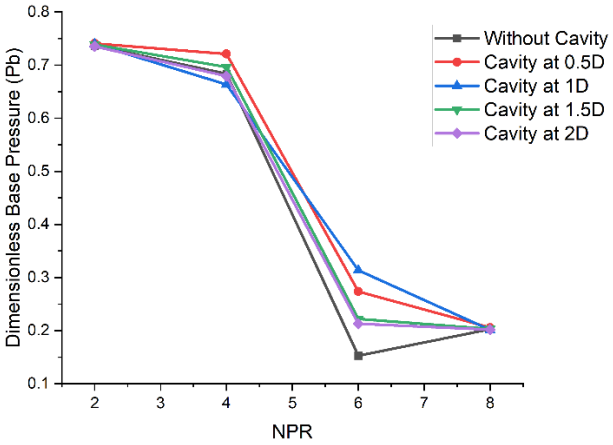

Fig. 24. Base pressure Vs NPR for Mach number 1.2 and L/D 5

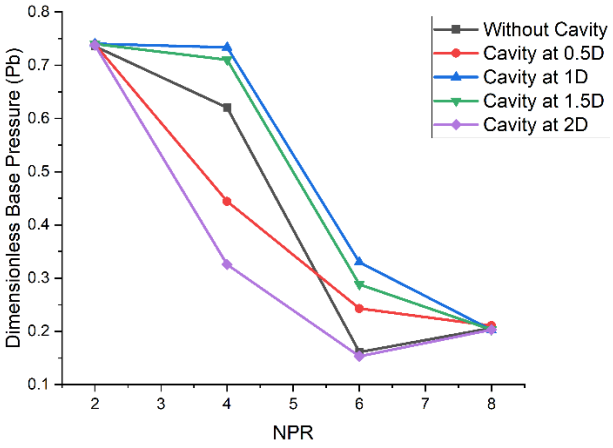

Fig. 25. Base pressure Vs NPR for Mach number 1.2 and L/D 6

3.3 Results: Base Pressure for Mach No. 1.4

Figure 26 to Figure 29 provide detailed insights into base pressure variations, considering various parameters such as nozzle pressure ratios, presence or absence of a cavity, and different cavity locations, all for a Mach number of 1.4.

The analysis from Figure 26 to Figure 29 underscores the strategic effectiveness of the cavity in influencing the base pressure. Specifically, at nozzle pressure ratios of four and six, the cavity demonstrates significant utility in modifying the base pressure. Notably, at a nozzle pressure ratio of six, the cavity consistently enhances the base pressure across all locations, including 0.5D, 1D, 1.5D, and 2D. Conversely, for nozzle pressure ratios of two and eight, the impact of the cavity on base pressure remains marginal, resulting in negligible differences in the outcomes.

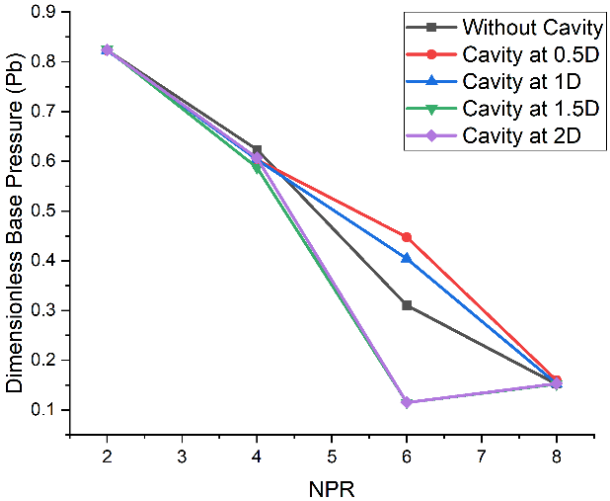

Fig. 26. Base pressure Vs NPR for Mach number 1.4 and L/D 3

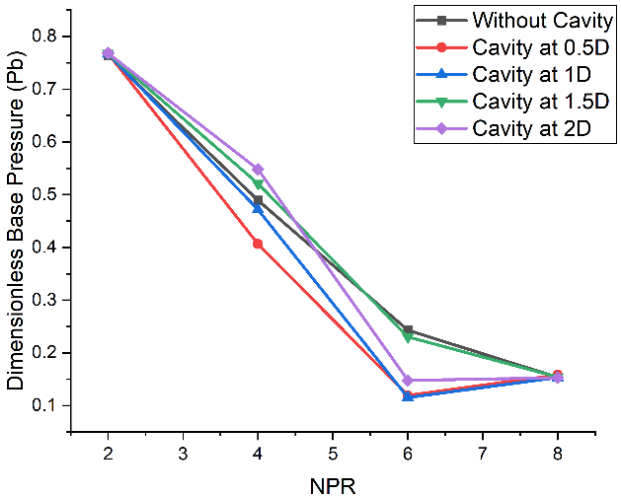

Fig. 27. Base pressure Vs NPR for Mach number 1.4 and L/D 4

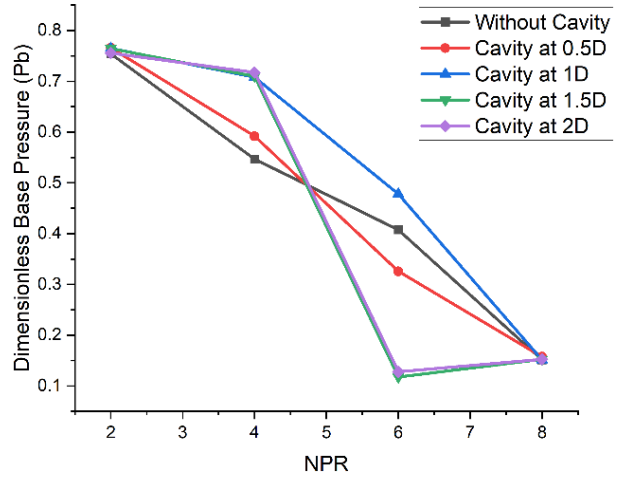

Fig. 28. Base pressure Vs NPR for Mach number 1.4 and L/D 5

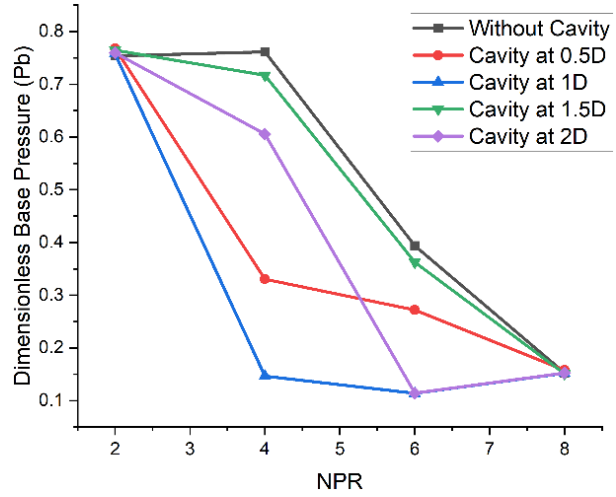

Fig. 29. Base pressure Vs NPR for Mach number 1.4 and L/D 6

3.4 Results: Base Pressure for Mach No. 1.6

Figure 30 to Figure 33 present detailed analyses of base pressure variations, incorporating parameters such as nozzle pressure ratios, presence or absence of a cavity, and different cavity locations, all for a Mach number of 1.6.

The observations derived from Figure 30 to Figure 33 emphasize the strategic role of the cavity in influencing the base pressure. Specifically, at nozzle pressure ratios of four, six, and eight, the cavity demonstrates notable efficacy in altering the base pressure. Notably, at a nozzle pressure ratio of six, the cavity exhibits significantly enhanced effectiveness in augmenting the base pressure. Conversely, at a nozzle pressure ratio of two, the impact of the cavity on base pressure remains minimal, resulting in negligible differences in the outcomes.

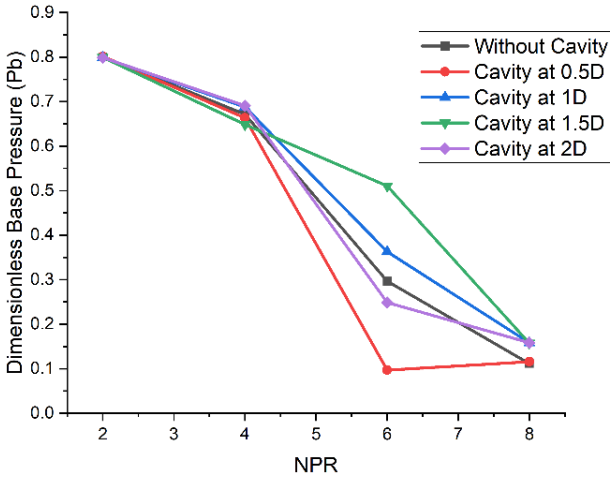

Fig. 30. Base pressure Vs NPR for Mach number 1.6 and L/D 3

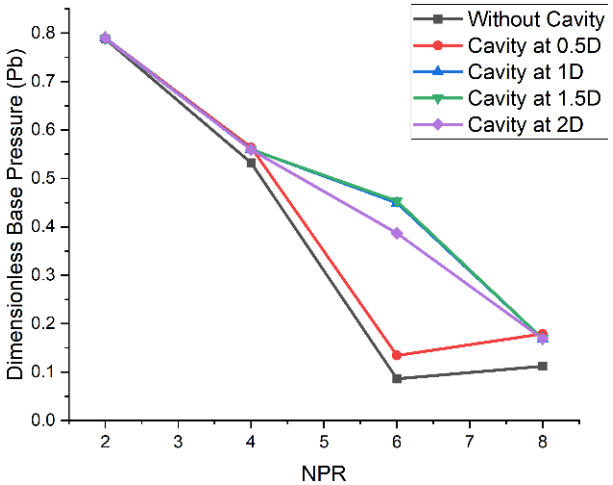

Fig. 31. Base pressure Vs NPR for Mach number 1.6 and L/D 4

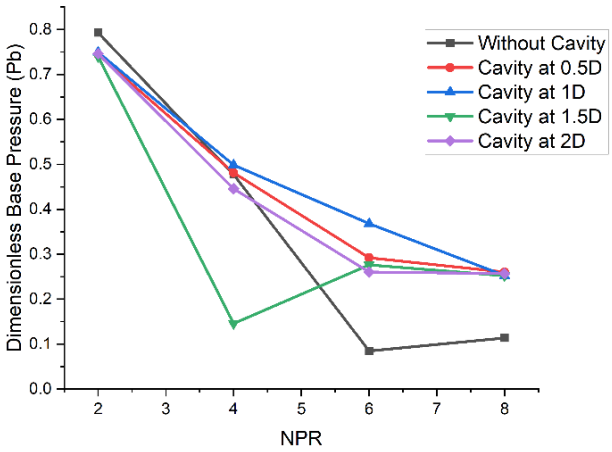

Fig. 32. Base pressure Vs NPR for Mach number 1.6 and L/D 5

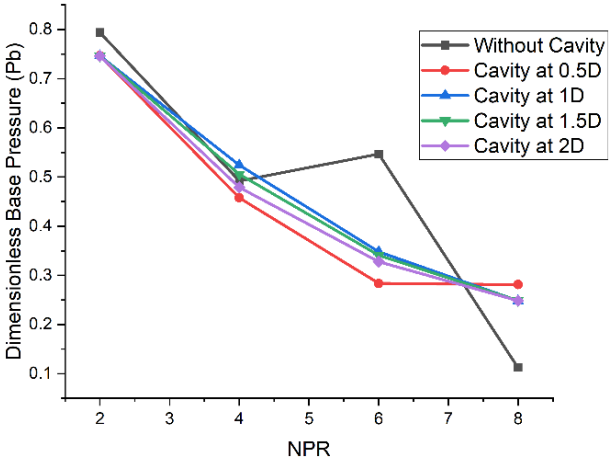

Fig. 33. Base pressure Vs NPR for Mach number 1.6 and L/D 6

3.5 Results: Base Pressure for Mach No. 1.8

Figure 34 to Figure 37 depict detailed analyses of base pressure interpretations, considering nozzle pressure ratios, the presence or absence of a cavity, and various cavity locations, all for a Mach number of 1.8.

The findings illustrated in Figure 34 to Figure 37 underscore the strategic significance of the cavity in influencing the base pressure. Specifically, at nozzle pressure ratios of six and eight, the cavity demonstrates notable efficacy in altering the base pressure. Particularly at a nozzle pressure ratio of six, the cavity exhibits significantly enhanced effectiveness in augmenting the base pressure, highlighting its critical role in this scenario.

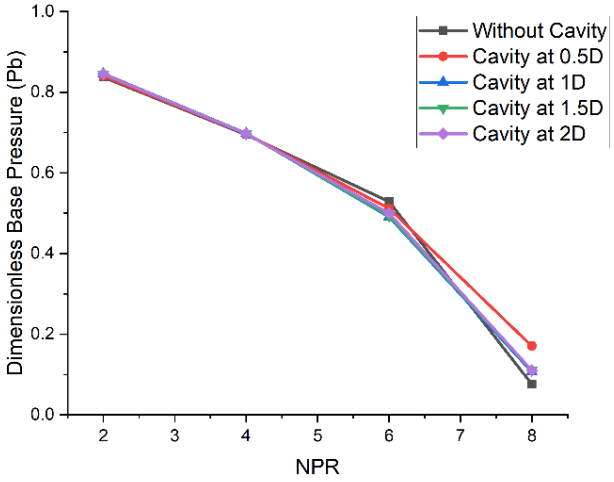

Fig. 34. Base pressure Vs NPR for Mach number 1.8 and L/D 3

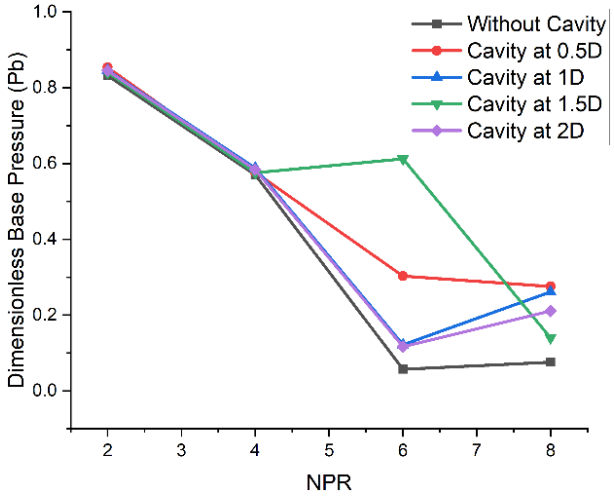

Fig. 35. Base pressure Vs NPR for Mach number 1.8 and L/D 4

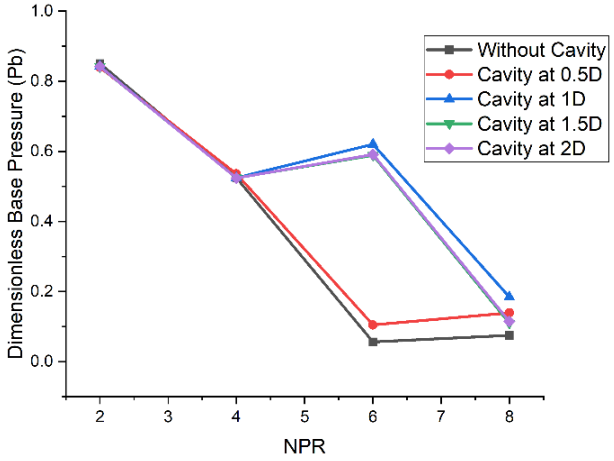

Fig. 36. Base pressure Vs NPR for Mach number 1.8 and L/D 5

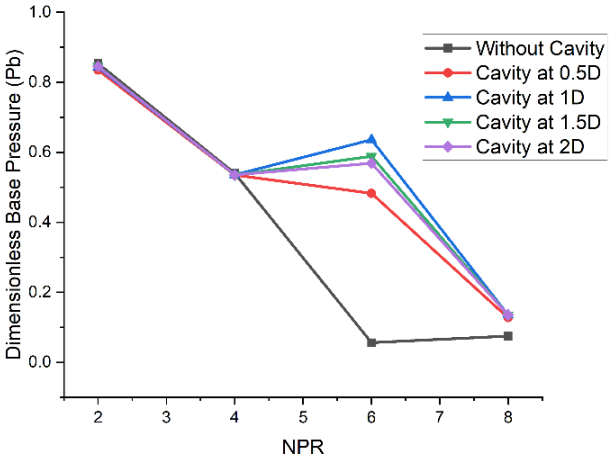

Fig. 37. Base pressure Vs NPR for Mach number 1.8 and L/D 6

3.6 Results: A Case Study Based on the Literature

The literature, particularly the work by Pandey and Rathakrishnan [31], presents a consistent trend in the results. For the research, three models without a cavity, with a cavity having an aspect ratio of 1, and with an aspect ratio of 2 were employed. Figure 38 displays the CFD and experimental outcomes for different length-to-diameter ratios. Notably, the trend observed in the CFD analysis results aligns closely with the experimental findings documented in the literature.

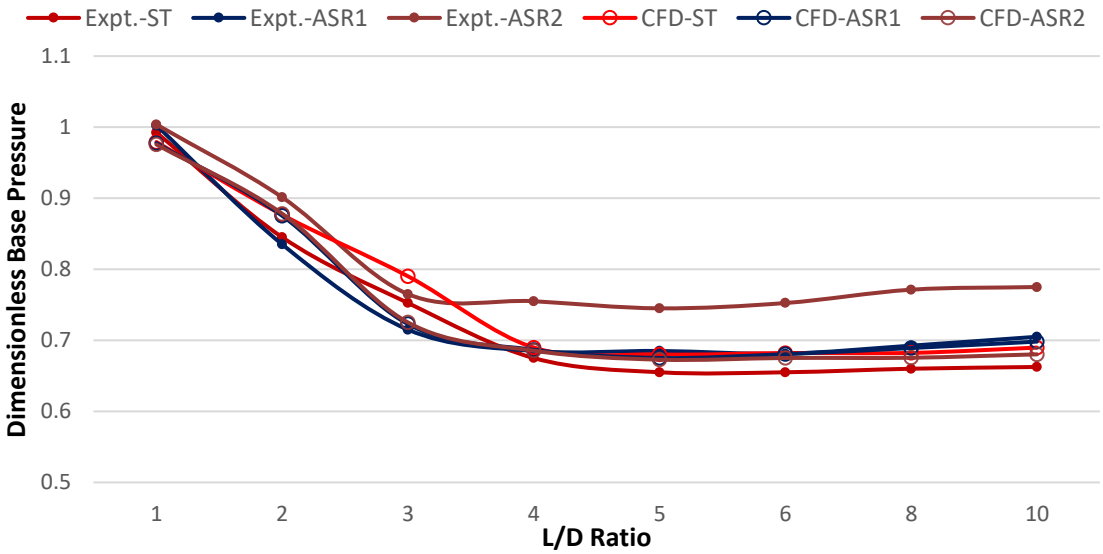

Fig. 38. CFD and experimental Result [31]

4. Conclusion

Based on the findings derived from this research, several significant conclusions can be drawn. The effectiveness of the cavity in manipulating the base pressure is notably demonstrated at NPR values of 4 and 6 for Mach numbers 1.2 and 1.4. This effectiveness arises from the strategic interaction between the cavity and the flow dynamics. Specifically, at NPR = 4 and 6, the cavity successfully influences the base pressure by intelligently engaging with the flow patterns in the enlarged duct after the cavity, resulting in a controlled pressure environment.

Conversely, the cavity is ineffective at NPR values of 2 and 8 for Mach numbers 1.2 and 1.4. This ineffectiveness can be attributed to specific flow behaviors: at NPR = 2, the flow reattaches to the enlarged duct post-cavity, rendering the cavity interaction negligible. Similarly, at NPR = 8, the flow reattaches to the enlarged duct before reaching the cavity, nullifying any impact the cavity might have on the flow dynamics and base pressure in the region of interest.

Further observations reveal the cavity's effectiveness in manipulating the base pressure at NPR values of 4, 6, and 8 for Mach numbers 1.6 and 1.8. In these cases, the cavity successfully interfaces with the flow reattachment points and the base region, orchestrating a controlled pressure environment conducive to the desired outcomes.

In summary, this study underscores the intricate relationship between cavity placement, NPR values, Mach numbers, and their collective influence on base pressure manipulation. The results provide invaluable insights into the nuanced interplay of these variables, offering crucial information for the optimization of duct designs in practical engineering applications.

References

[1] Pesce, Vincenzo, Stefano Silvestrini, and Michèle Lavagna. "Radial basis function neural network aided adaptive extended Kalman filter for spacecraft relative navigation." *Aerospace Science and Technology* 96 (2020): 105527. https://doi.org/10.1016/j.ast.2019.105527

[2] Pathan, Khizar Ahmed, Prakash S. Dabeer, and Sher Afghan Khan. "Investigation of base pressure variations in internal and external suddenly expanded flows using CFD analysis." *CFD Letters* 11, no. 4 (2019): 32-40.

[3] Khan, Sher Afghan, M. A. Fatepurwala, K. N. Pathan, and P. S. Dabeer, and Maughal Ahmed Ali Baig. "CFD analysis of human powered submarine to minimize drag." *International Journal of Mechanical and Production Engineering Research and Development* 8, no. 3 (2018): 1057-1066. https://doi.org/10.24247/ijmperdjun2018111

[4] Pathan, Khizar A., Sher A. Khan, N. A. Shaikh, Arsalan A. Pathan, and Shahnawaz A. Khan. "An investigation of boat-tail helmet to reduce drag." *Advances in Aircraft and Spacecraft Science* 8, no. 3 (2021): 239-250.

[5] Pathan, Khizar Ahmed, Syed Ashfaq, Prakash S. Dabeer, and Sher Afgan Khan. "Analysis of parameters affecting thrust and base pressure in suddenly expanded flow from nozzle." *Journal of Advanced Research in Fluid Mechanics and Thermal Sciences* 64, no. 1 (2019): 1-18.

[6] Pathan, Khizar Ahmed, Prakash S. Dabeer, and Sher Afghan Khan. "Influence of expansion level on base pressure and reattachment length." *CFD Letters* 11, no. 5 (2019): 22-36.

[7] Pathan, Khizar A., Prakash S. Dabeer, and Sher A. Khan. "Enlarge duct length optimization for suddenly expanded flows." *Advances in Aircraft and Spacecraft Science* 7, no. 3 (2020): 203-214.

[8] Pathan, Khizar Ahmed, Prakash S. Dabeer, and Sher Afghan Khan. "Optimization of area ratio and thrust in suddenly expanded flow at supersonic Mach numbers." *Case Studies in Thermal Engineering* 12 (2018): 696-700. https://doi.org/10.1016/j.csite.2018.09.006

[9] Pathan, Khizar Ahmed, Sher Afghan Khan, and P. S. Dabeer. "CFD analysis of effect of flow and geometry parameters on thrust force created by flow from nozzle." In *2017 2nd International Conference for Convergence in Technology (I2CT)*, pp. 1121-1125. IEEE, 2017. https://doi.org/10.1109/I2CT.2017.8226302

[10] Pathan, Khizar Ahmed, Sher Afghan Khan, and P. S. Dabeer. "CFD analysis of effect of area ratio on suddenly expanded flows." In *2017 2nd International Conference for Convergence in Technology (I2CT)*, pp. 1192-1198. IEEE, 2017. https://doi.org/10.1109/I2CT.2017.8226315

[11] Pathan, Khizar Ahmed, Sher Afghan Khan, and P. S. Dabeer. "CFD analysis of effect of Mach number, area ratio and nozzle pressure ratio on velocity for suddenly expanded flows." In *2017 2nd International Conference for Convergence in Technology (I2CT)*, pp. 1104-1110. IEEE, 2017. https://doi.org/10.1109/I2CT.2017.8226299

[12] Khan, Ambareen, Nurul Musfirah Mazlan, and Mohd Azmi Ismail. "Analysis of flow through a convergent nozzle at Sonic Mach Number for Area Ratio 4." *Journal of Advanced Research in Fluid Mechanics and Thermal Sciences* 62, no. 1 (2019): 66-79.

[13] Khan, Ambareen, Parvathy Rajendran, and Junior Sarjit Singh Sidhu. "Passive control of base pressure: a review." *Applied Sciences* 11, no. 3 (2021): 1334. https://doi.org/10.3390/app11031334

[14] Khan, Ambareen, Nurul Musfirah Mazlan, and Ervin Sulaeman. "Effect of Ribs as Passive Control on Base Pressure at Sonic Mach Numbers." *CFD Letters* 14, no. 1 (2022): 140-151. https://doi.org/10.37934/cfdl.14.1.140151

[15] Pathan, Khizar Ahmed, Prakash S. Dabeer, and Sher Afghan Khan. "An investigation to control base pressure in suddenly expanded flows." *International Review of Aerospace Engineering (IREASE)* 11, no. 4 (2018): 162-169. https://doi.org/10.15866/irease.v11i4.14675

[16] Khan, Sher Afghan, and E. Rathakrishnan. "Active control of base pressure in supersonic regime." *Journal of Aerospace Engineering, Institution of Engineers, India* 87 (2006): 1-8.
[17] Shaikh, Javed S., Krishna Kumar, Khizar A. Pathan, and Sher A. Khan. "Analytical and computational analysis of pressure at the nose of a 2D wedge in high speed flow." *Advances in Aircraft and Spacecraft Science* 9, no. 2 (2022): 119-130.
[18] Shaikh, Sohel Khalil, Khizar Ahmed Pathan, Zakir Ilahi Chaudhary, B. G. Marlpalle, and Sher Afghan Khan. "An Investigation of Three-Way Catalytic Converter for Various Inlet Cone Angles Using CFD." *CFD Letters* 12, no. 9 (2020): 76-90. https://doi.org/10.37934/cfdl.12.9.7690
[19] Shaikh, Sohel Khalil, Khizar Ahmed Pathan, Zakir Ilahi Chaudhary, and Sher Afghan Khan. "CFD analysis of an automobile catalytic converter to obtain flow uniformity and to minimize pressure drop across the monolith." *CFD Letters* 12, no. 9 (2020): 116-128. https://doi.org/10.37934/cfdl.12.9.116128
[20] Khan, Sher Afghan, Abdul Aabid, and Ahamed Saleel Chandu Veetil. "CFD simulation with analytical and theoretical validation of different flow parameters for the wedge at supersonic Mach number." *International Journal of Mechanical and Mechatronics Engineering* 19, no. 1 (2019): 170-177.
[21] Sajali, Muhammad Fahmi Mohd, Abdul Aabid, Sher Afghan Khan, Fharukh Ahmed Ghasi Mehaboobali, and Erwin Sulaeman. "Numerical Investigation of Flow Field of a Non-Circular Cylinder." *CFD Letters* 11, no. 5 (2019): 37-49.
[22] Khan, Sher Afghan, Mohammed Asadullah, G. M. Fharukh Ahmed, Ahmed Jalaluddeen, and Maughal Ahmed Ali Baig. "Passive control of base drag in compressible subsonic flow using multiple cavity." *International Journal of Mechanical and Production Engineering Research and Development* 8, no. 4 (2018): 39-44. https://doi.org/10.24247/ijmperdaug20185
[23] Khan, Sher Afghan, Mohammed Asadullah, and Jafar Sadhiq. "Passive control of base drag employing dimple in subsonic suddenly expanded flow." *International Journal of Mechanical & Mechatronics Engineering* 18, no. 3 (2018): 69-74.
[24] Khan, Ambareen, Parvathy Rajendran, Junior Sarjit Singh Sidhu, S. Thanigaiarasu, Vijayanandh Raja, and Qasem Al-Mdallal. "Convolutional neural network modeling and response surface analysis of compressible flow at sonic and supersonic Mach numbers." *Alexandria Engineering Journal* 65 (2023): 997-1029. https://doi.org/10.1016/j.aej.2022.10.006
[25] Shamitha, Shamitha, Asha Crasta, Khizer Ahmed Pathan, and Sher Afghan Khan. "Numerical simulation of surface pressure of a wedge at supersonic Mach numbers and application of design of experiments." *Journal of Advanced Research in Applied Mechanics* 101, no. 1 (2023): 1-18. https://doi.org/10.37934/aram.101.1.118
[26] Shamitha, Shamitha, Asha Crasta, Khizar Ahmed Pathan, and Sher Afghan Khan. "Analytical and Numerical Simulation of Surface Pressure of an Oscillating Wedge at Hypersonic Mach Numbers and Application of Taguchi's Method." *Journal of Advanced Research in Applied Sciences and Engineering Technology* 30, no. 1 (2023): 15-30. https://doi.org/10.37934/araset.30.1.1530
[27] Shaikh, Javed S., Krishna Kumar, Khizar A. Pathan, and Sher A. Khan. "Computational Analysis of Surface Pressure Distribution over a 2D Wedge in the Supersonic and Hypersonic Flow Regimes." *Fluid Dynamics & Materials Processing* 19, no. 6 (2023). https://doi.org/10.32604/fdmp.2023.025113
[28] Shaikh, Javed Shoukat, Khizar Ahmed Pathan, Krishna Kumar, and Sher Afghan Khan. "Effectiveness of Cone Angle on Surface Pressure Distribution along Slant Length of a Cone at Hypersonic Mach Numbers." *Journal of Advanced Research in Fluid Mechanics and Thermal Sciences* 104, no. 1 (2023): 185-203. https://doi.org/10.37934/arfmts.104.1.185203
[29] Pathan, Khizar, Prakash Dabeer, and Khan Sher. "An investigation of effect of control jets location and blowing pressure ratio to control base pressure in suddenly expanded flows." *Journal of Thermal Engineering* 6, no. 2 (2019): 15-23. https://doi.org/10.18186/thermal.726106
[30] Pathan, Khizar Ahmed, Prakash S. Dabeer, and Sher Afghan Khan. "Effect of nozzle pressure ratio and control jets location to control base pressure in suddenly expanded flows." *Journal of Applied Fluid Mechanics* 12, no. 4 (2019): 1127-1135. https://doi.org/10.29252/jafm.12.04.29495
[31] Pandey, K. M., and E. Rathakrishnan. "Annular cavities for Base flow control." *International Journal of Turbo and Jet Engines* 23, no. 2 (2006): 113-128. https://doi.org/10.1515/TJJ.2006.23.2.113